

# <sup>1</sup> SNAzzy: an image processing pipeline for investigating global Synchronous Network Activity

<sup>3</sup> **Carlos D. Paiva**  <sup>1,2</sup>, **Alana J. Evora**  <sup>1,2</sup>, **Shirui Zheng**  <sup>1,2</sup>, and **Arnaldo Carreira-Rosario**  <sup>1,2</sup>

<sup>5</sup> **1** Department of Biology, Duke University, Durham, NC 27708 **2** Department of Neurobiology, Duke University, Durham, NC 27708 ¶ Corresponding author

DOI: [10.xxxxxx/draft](https://doi.org/10.xxxxxx/draft)

## Software

- [Review](#) ↗
- [Repository](#) ↗
- [Archive](#) ↗

Editor: ↗

Submitted: 06 November 2025

Published: unpublished

## License

Authors of papers retain copyright and release the work under a Creative Commons Attribution 4.0 International License ([CC BY 4.0](https://creativecommons.org/licenses/by/4.0/))

## <sup>7</sup> Summary

<sup>8</sup> Genetically encoded fluorescent indicators are powerful tools for monitoring biological processes in live samples ([Lin & Schnitzer, 2016](#); [Nakai et al., 2001](#)). When combined with a large field of view, a single time-lapse recording has the potential to capture many specimens, facilitating high-throughput data collection. However, this approach generates large, multidimensional datasets that are challenging to process and analyze. We present SNAzzy, a Python package for studying synchronous network activity (SNA) in *Drosophila* embryos via high-throughput microscopy. SNA is a hallmark of developing nervous systems ([Akin & Zipursky, 2020](#); [Blankenship & Feller, 2009](#); [Wu et al., 2024](#)), often studied using genetically encoded calcium indicators to monitor neural activity *in vivo*. SNAzzy processes and analyzes time-lapse datasets taken from live samples using fluorescent widefield microscopy. Each dataset contains dozens of individual specimens in the same field of view and thousands of time points. The software offers individual specimen cropping for optimization of storage and processing, adaptive regions of interest for quantification of fluorescence and changes in morphology over time, a custom peak detection algorithm, and a graphical user interface for data visualization, curation, and dataset comparison. This tool can be readily applied to analyze fluorescent intensities in time-lapse microscopy experiments that involve simultaneous imaging of multiple samples, particularly small-sized specimens ([Avasthi et al., 2023](#); [Donouhe et al., 2018](#)).

## <sup>25</sup> Statement of need

<sup>26</sup> During synchronous network activity (SNA), many neurons fire simultaneously, generating waves of activity that span across large portions of the nervous system ([Akin & Zipursky, 2020](#); [Blankenship & Feller, 2009](#); [Wu et al., 2024](#)). In *Drosophila* embryos, SNA typically lasts 4 hours, during which the nervous system undergoes a stereotyped morphological change via ventral nerve cord condensation ([Carreira-Rosario et al., 2021](#); [Crisp et al., 2008](#); [Karkali et al., 2022](#)). To gain an understanding of SNA, it is essential to quantify waves of activity in the nervous system while also tracking morphology as a proxy for neurodevelopment. For these reasons, we combine a commonly used genetically encoded calcium indicator (GECI) that reports neural activity with a structural fluorophore ([Carreira-Rosario et al., 2021](#)). The structural fluorophore signal remains stable, independent of neural activity, making it suitable for continuous tracking morphology of the nerve cord. To record many embryos during SNA, we use a wide-field fluorescence microscopy system that captures the GECI and structural fluorophore signal of dozens of developing embryos for over 5 hours.

<sup>39</sup> We were unable to find a tool designed for widefield microscopy that rapidly processes multiple specimens, quantifies levels of fluorophore activity, and incorporates a peak-finding algorithm suitable for global calcium traces. SNAzzy is designed to investigate global levels of neural

42 activity across multiple developing embryos simultaneously.

43 **Tracking of multiple “adaptive ROIs”**

44 To the best of our knowledge, there are no other packages that provide functionality for  
45 automated parsing of raw images of many live specimens into activity and morphological  
46 quantifications. Other studies have employed manual selection of regions of interest (ROIs)  
47 and used static ROIs (Akin & Zipursky, 2020; Ardiel et al., 2022; Carreira-Rosario et al.,  
48 2021; Menzies et al., 2024). Manual selection often generates imprecise ROIs, which can  
49 lead to inaccurate quantifications, and is also cumbersome and prone to human error. Static  
50 ROIs are not reliable for detecting the fluorescent signal of live specimens that change in  
51 morphology and move while imaging. SNAzzy fills these gaps as an accessible pipeline for the  
52 automated analysis of multiple live samples in parallel. The pipeline generates an “adaptive  
53 ROI” that changes frame-by-frame for each specimen. This enables the accurate tracking of  
54 fluorescence intensity as well as changes in tissue morphology or size. SNAzzy’s design provides  
55 an automated, modular, and fully auditable workflow, and ultimately contributes to more  
56 reproducible and comparable results across experiments.

57 **Capturing global Calcium dynamics**

58 To the best of our knowledge, there are no open-source packages that provide tools for  
59 performing automated data analysis and quantification of global calcium dynamics. Most open-  
60 source tools available for analyzing neural activity using GECI focus on segmenting individual  
61 neurons within a single specimen. CaImAn (Giovannucci et al., 2019), and Suite2p (Pachitariu  
62 et al., 2016) are among the most widely used. These packages detect calcium dynamics and use  
63 individual neuron statistics to perform spike inference, but do not offer direct peak detection  
64 on the calcium signal. Furthermore, they are optimized for two-photon microscopy as opposed  
65 to wide-field microscopy. SNAzzy provides a series of automated analyses and quantifications  
66 to analyze global calcium levels in time-series acquired with widefield microscopes.

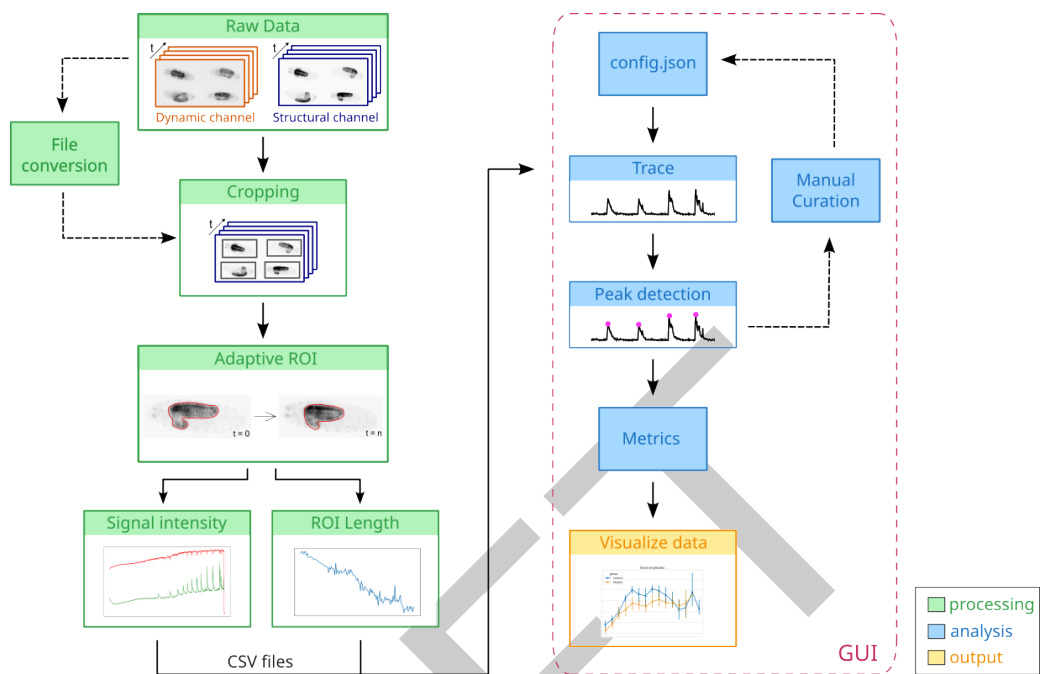


**Figure 1: Schematic of the SNAzzy pipeline.** Time-lapse taken from fluorescent widefield microscopes (raw data) enters the processing stage (green). The processing stage outputs two types of CSV files: time series of signal intensities from each recorded channel and ROI length. CSV files enter the analysis stage (blue) to generate normalized fluorescent traces and detect peaks along with other signal processing metrics. These initial traces can be visualized to curate the data. Curation generates a configuration file that works as metadata across platforms and users. Curated data can be reanalyzed and used to visualize final data and compare across groups (yellow). Analysis and output stages are performed in the GUI (red dashed box), along with other metrics. Dashed arrows indicate optional steps.

## 67 Pipeline Description

- 68 The initial input for SNAzzy [Figure 1](#) is raw time-lapse imaging data containing multiple  
69 embryos. Each embryo expresses a GECL (dynamic fluorophore) and a structural fluorophore.  
70 Fluorophores are imaged in different optical channels.
- 71 The first pipeline step converts the raw data to TIF format, thereby avoiding compatibility  
72 issues that may arise when parsing different proprietary formats [Figure 1](#). All embryos are then  
73 segmented using histogram equalization, followed by intensity threshold binarization ([Otsu,](#)  
74 [1979](#)). Boxes surrounding the segments are cropped into individual time-lapses for each embryo.  
75 Cropping results in a substantial memory reduction, as most background pixels are removed,  
76 with cropped images typically accounting for around 40% of the original size.
- 77 The next step is to process each individual specimen. First, the ROI, which in our case is  
78 the entire central nervous system (CNS), is defined by binarizing the structural channel and  
79 selecting the largest connected component. This process is repeated at every time point to  
80 generate an “adaptive ROI”. From these adaptive ROI, the average signal intensity for both  
81 channels is extracted. The results are saved as CSV files and are the basis for downstream  
82 analysis.

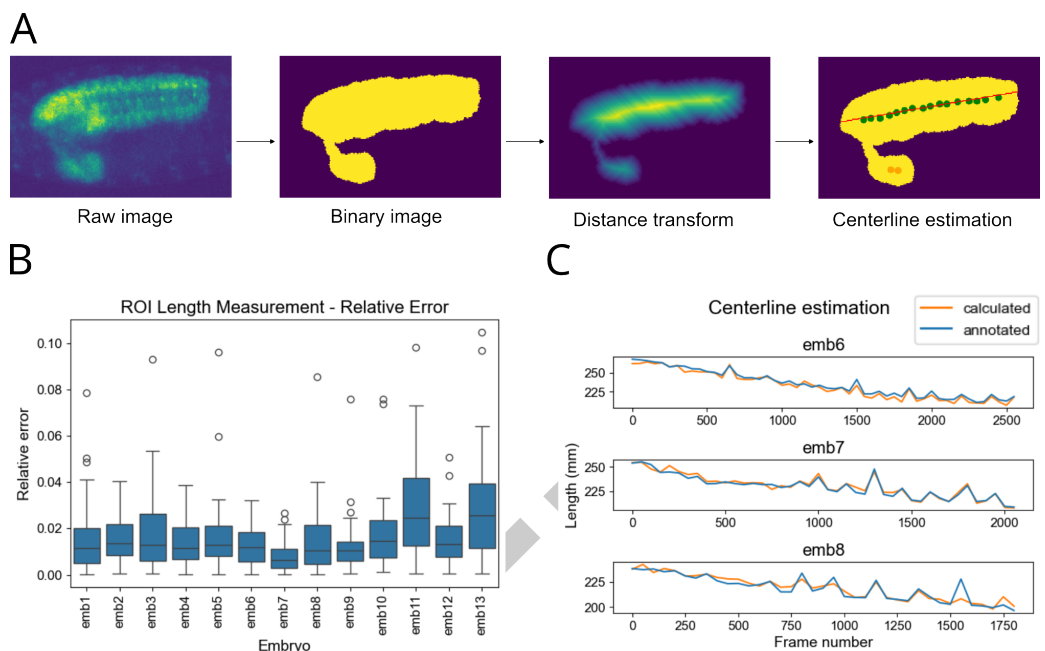


**Figure 2: ROI length measurement algorithm and validation.** A) Steps to calculate the ROI length. The ROI length is calculated by estimating the centerline (red line) using points of maximum (dots) in the distance transform, followed by RANSAC to ignore outliers (orange dots). B) Validation of the method as relative error (measured - annotated) / annotated. Each whisker bar summarizes the relative error for frames taken at intervals of 50 timepoints. C) Comparison of absolute values over a time series for three representative embryos.

83 The ROI is also used to measure the length of the CNS [Figure 2](#). Drosophila embryo CNS  
84 length serves as an internal proxy for neurodevelopmental stages, enabling more accurate  
85 comparisons across embryos ([Carreira-Rosario et al., 2021](#)). The CNS length is calculated by  
86 centerline estimation. First, a distance transform is applied to the binarized image, and local  
87 maxima points are detected. Depending on the embryo's orientation, some points may be part  
88 of the brain lobes and must be filtered out to accurately measure the CNS length. To obtain a  
89 robust centerline estimate that can ignore outliers, we use RANSAC ([Fischler & Bolles, 1981](#))  
90 over the local maxima points and measure the overlap between the fitted line and the binary  
91 image. CNS length is also detected frame by frame and exported as a CSV file [Figure 1](#).

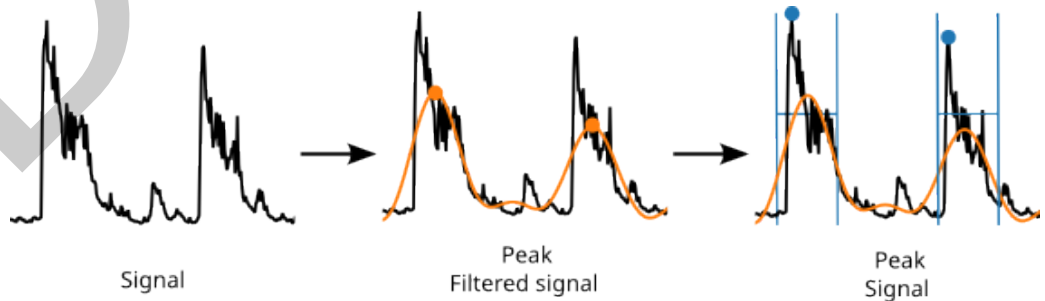


**Figure 3: Peak detection algorithm.** A low-pass filter (orange line) is applied to the  $\Delta F/F$  signal (black line) to remove fast transients. The peak in the filtered signal (orange dot) is then ported back to the  $\Delta F/F$  (blue dot) signal by selecting the leftmost peak within a search window (blue lines).

92 The package utilizes average signal intensity measurements to calculate  $\Delta F/F$  traces and peaks.  
93 For  $\Delta F/F$ , we first calculate the ratiometric signal (dynamic signal / structural signal) and

94 then its baseline, which is defined as the average of the N lowest values within a sliding window.  
 95 The generated  $\Delta F/F$  traces contain long-duration bouts of activity with superimposed fast  
 96 transients [Figure 3](#). The former represents the bursts of activity and is the most relevant for  
 97 the initial analysis. To mark only these more prolonged bouts, we apply a low-pass frequency  
 98 filter to omit transients. Peaks in the filtered trace are detected using SciPy ([Virtanen et al.,](#)  
 99 [2020](#)). Finally, the detected peaks are ported to the original  $\Delta F/F$  signal.

100 Results can be visualized and curated in a graphical user interface (GUI) implemented in PyQt6  
 101 [Figure 4](#). During curation, researchers can modify data analysis parameters, which are persisted  
 102 in a JSON configuration file and utilized by the core analysis code across different machines  
 103 and users. Finally, a large number of different metrics and representations derived from  $\Delta F/F$ ,  
 104 CNS length, and peaks can be visualized and plotted using the GUI. These include SNA onset,  
 105 burst duration and spectrograms, among others.

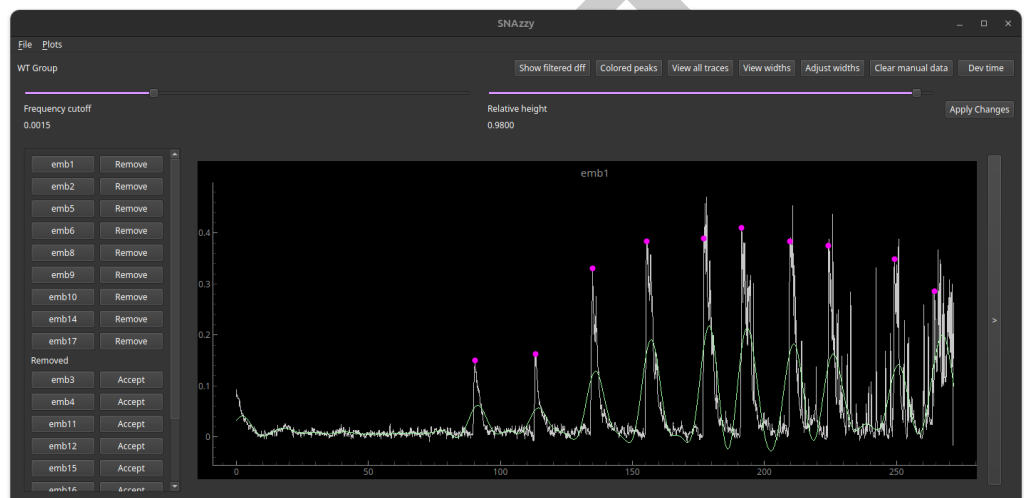


**Figure 4: GUI for data validation, curation, visualization and plotting.** Initial GUI screen. A  $\Delta F/F$  trace (white) and the corresponding peaks (magenta dots) are shown. The low-passed signal (green line) is used as a reference to determine peaks. The GUI enables the modification of analysis parameters, visualization of data, and comparison of metrics across groups of experiments, as well as manual adjustment of peak data.

## 106 Conclusion

107 In conclusion, genetically encoded fluorescent indicators and microscopy systems are evolving  
 108 rapidly, increasing the data acquisition throughput. Custom open-source tools are needed to  
 109 handle such large data files. SNAZZY addresses this by offering an automated, scalable, and  
 110 user-friendly platform for analyzing synchronous network activity in developing embryos. As an  
 111 open and versatile solution, SNAZZY offers tools for a broader range of applications in time-lapse  
 112 fluorescence imaging across diverse biological systems.

## 113 Acknowledgments

114 We acknowledge Newton PenkoffLidbeck and D. Berfin Azizoglu for feedback on the manuscript.  
 115 This work was partially funded by NINDS and the BRAIN initiative (R00NS119295).

## 116 References

- 117 Akin, O., & Zipursky, S. L. (2020). Activity regulates brain development in the fly. *Current  
118 Opinion in Genetics & Development*, 65, 8–13. <https://doi.org/10.1016/j.gde.2020.04.005>
- 119 Ardiel, E. L., Lauziere, A., Xu, S., Harvey, B. J., Christensen, R. P., Nurrish, S., Kaplan, J.  
120 M., & Shroff, H. (2022). Stereotyped behavioral maturation and rhythmic quiescence in *c.*  
121 *Elegans* embryos. *eLife*, 11. <https://doi.org/10.7554/eLife.76836>
- 122 Avasthi, P., Essock-Burns, T., Garcia, I., Galo, Gehring, J., Matus, D. Q., Mets, D. G., &  
123 York, R. (2023). *Gotta catch 'em all: Agar microchambers for high-throughput single-cell  
124 live imaging*. <https://doi.org/10.57844/arcadia-v1bg-6b60>
- 125 Blankenship, A. G., & Feller, M. B. (2009). Mechanisms underlying spontaneous patterned  
126 activity in developing neural circuits. *Nature Reviews Neuroscience*, 11(1), 18–29.  
127 <https://doi.org/10.1038/nrn2759>
- 128 Carreira-Rosario, A., York, R. A., Choi, M., Doe, C. Q., & Clandinin, T. R. (2021). Mechanosensi-  
129 sory input during circuit formation shapes *drosophila* motor behavior through patterned  
130 spontaneous network activity. *Current Biology: CB*, 31(23), 5341–5349.e4. <https://doi.org/10.1016/j.cub.2021.08.022>
- 132 Crisp, S., Evers, J. F., Fiala, A., & Bate, M. (2008). *The development of motor coordination  
133 in drosophila embryos*. 3717, 3707–3717. <https://doi.org/10.1242/dev.026773>
- 134 Donoughe, S., Kim, C., & Extavour, C. G. (2018). High-throughput live-imaging of embryos  
135 in microwell arrays using a modular specimen mounting system. *Biology Open*, 7(7),  
136 bio031260. <https://doi.org/10.1242/bio.031260>
- 137 Fischler, M. A., & Bolles, R. C. (1981). Random sample consensus: A paradigm for model  
138 fitting with applications to image analysis and automated cartography. *Communications of  
139 the ACM*, 24(6), 381–395. <https://doi.org/10.1145/358669.358692>
- 140 Giovannucci, A., Friedrich, J., Gunn, P., Kalfon, J., Brown, B. L., Koay, S. A., Taxidis, J.,  
141 Najafi, F., Gauthier, J. L., Zhou, P., Khakh, B. S., Tank, D. W., Chklovskii, D. B., &  
142 Pnevmatikakis, E. A. (2019). CalmAn an open source tool for scalable calcium imaging  
143 data analysis. *eLife*, 8. <https://doi.org/10.7554/eLife.38173>
- 144 Karkali, K., Tiwari, P., Singh, A., Tlili, S., Jorba, I., Navajas, D., Muñoz, J. J., Saunders, T. E.,  
145 & Martin-Blanco, E. (2022). Condensation of the *drosophila* nerve cord is oscillatory and  
146 depends on coordinated mechanical interactions. *Developmental Cell*, 57(7), 867–882.e5.  
147 <https://doi.org/10.1016/j.devcel.2022.03.007>
- 148 Lin, M. Z., & Schnitzer, M. J. (2016). Genetically encoded indicators of neuronal activity.  
149 *Nature Neuroscience*, 19(9), 1142–1153. <https://doi.org/10.1038/nn.4359>
- 150 Menzies, J. A. C., Chagas, A. M., Baden, T., & Alonso, C. R. (2024). A microRNA that controls  
151 the emergence of embryonic movement. In *eLife*. <https://doi.org/10.7554/elife.95209.2>
- 152 Nakai, J., Ohkura, M., & Imoto, K. (2001). A high signal-to-noise  $Ca^{2+}$  probe composed  
153 of a single green fluorescent protein. *Nature Biotechnology*, 19(2), 137–141. <https://doi.org/10.1038/84397>
- 155 Otsu, N. (1979). A threshold selection method from gray-level histograms. *IEEE Transactions  
156 on Systems, Man, and Cybernetics*, 9(1), 62–66. <https://doi.org/10.1109/TSMC.1979.4310076>
- 158 Pachitariu, M., Stringer, C., Dipoppa, M., Schröder, S., Rossi, L. F., Dalgleish, H., Carandini,  
159 M., & Harris, K. D. (2016). Suite2p: Beyond 10,000 neurons with standard two-photon  
160 microscopy. In *bioRxiv* (p. 061507). bioRxiv. <https://doi.org/10.1101/061507>
- 161 Virtanen, P., Gommers, R., Oliphant, T. E., Haberland, M., Reddy, T., Cournapeau, D.,

<sup>162</sup> Burovski, E., Peterson, P., Weckesser, W., Bright, J., Walt, S. J. van der, Brett, M.,  
<sup>163</sup> Wilson, J., Millman, K. J., Mayorov, N., Nelson, A. R. J., Jones, E., Kern, R., Larson, E., ...  
<sup>164</sup> Contributors, S. 1.0. (2020). SciPy 1.0: Fundamental algorithms for scientific computing  
<sup>165</sup> in python. *Nature Methods*, 17(3), 261–272. <https://doi.org/10.1038/s41592-019-0686-2>

<sup>166</sup> Wu, M. W., Kourdougli, N., & Portera-Cailliau, C. (2024). Network state transitions dur-  
<sup>167</sup> ing cortical development. *Nature Reviews. Neuroscience*. <https://doi.org/10.1038/s41583-024-00824-y>

DRAFT